Deployable, Collapsible, Rigid Origami Shelter

Lia Coleman, George Pantazis, and Noa Machover

May 18, 2017

Figure 1: Final assembled dome construction, 1m diameter.

Contents

Abstract

For our project, our aim was to explore various methods for constructing rigid, collapsible, deployable origami shelters. First, we explored a method of combining a Hoberman Sphere with a Flasher so that the two systems could be deployed simultaneously. However, we performed a volume-compression analysis, and found that an umbrella has a significantly better compression ratio. We reverse-engineered an umbrella to discern its crease pattern. We then adjusted the crease pattern and tailored it to be able to fold into our desired 3D shape, a hemisphere. However, we believe that our crease pattern and equations could easily be adjusted to approximate many 3D convex surfaces. We wrote a Matlab script to perform the angle and length calculations for the crease pattern. Our final crease pattern had a volume-compression ratio of 2.1%, which is better than the Hoberman sphere (an average of 4.6%) and very close to the ShedRain umbrella (1.3%). As a proof of concept, we constructed a 1 meter diameter shelter out of 1/16" acrylic and vinyl.

1 Introduction

Foldable shelters allow for compaction and transportability. This compaction along with quick and simple deployment allows for applications in temporary shelters for refugees or the homeless. We each came to this project with different backgrounds and interests. George was particularly interested in modes of deployment for rigid structures. Lia was interested in the problem of transforming a 2D sheet into a desired 3D form using as little glue or nails or other additional nonessential materials as possible– a valuable skill for construction of anything in general. Noa was interested in the architecture, spatial qualities, and social implications of foldable, portable shelters as well as the potential for a customizable, modular design.

2 Previous Work and Inspiration

2.1 Previous Folding Shelters

Origami has long been an inspiration for architects in the creation of inhabitable spaces. We investigated previous projects involving foldable shelters and identified two broad categories of interest:

1. Flat-folded structures that deploy from a 2D structure into a 3D structure (further examples).

   Generally type 1 structures can be further classified in two sub categories:

   (a) A hinged 2D shape that folds along edges to form an enclosed polyhedron, as seen in Figure 2 [Kim11].

Figure 2: Hwang Kim, urban homeless cocoon. Hinged 2D shape that folds along edges to form enclosed polyhedron.

(b) A 2D polygonal shape that traces some curve in 3D hence enclosing a volume. A great example of this is Tomohiro Tachi's "architectural origami" building connector in Figure 3 [Tac].

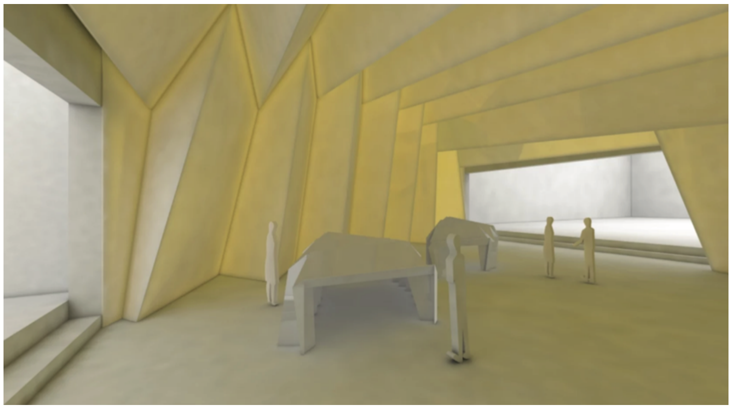

Figure 3: Tomohiro Tachi, Architectural Building Connector.

2. Volume compression structures that deploy from compressed 3D structures into larger 3D structures (examples include compact umbrellas and Hoberman Spheres).

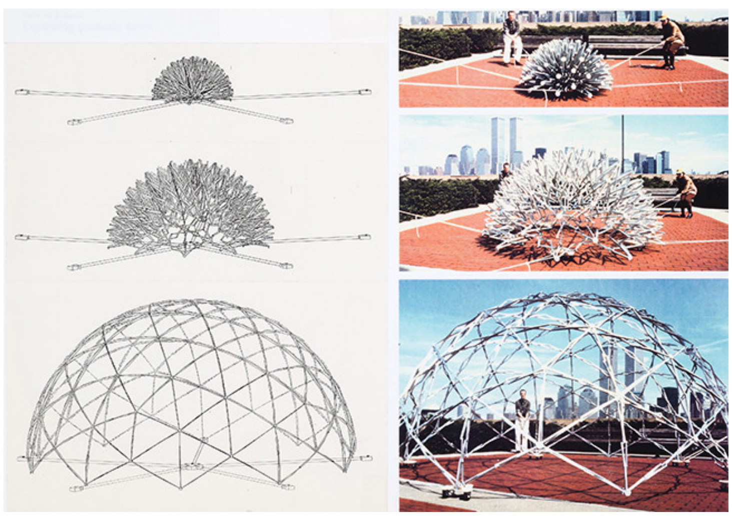

Figure 4: Hoberman Sphere structures.

Type 1 Structures - although folding flat - will generally have a larger footprint when undeployed making them slightly more cumbersome for one-person carrying unless they can be split into individual pieces that are then joined.

We sought to build a type 2 structure that could reasonably fit in a back-pack sized volume while still deploying to a size able to accommodate at least one person.

2.2 Design elements

In Type 1, we have been particularly inspired by Miura folds, as shown in Figure 5. We drew inspiration from the fact that Miura folds can be made to approximate curved surfaces, as shown in Figure 6 [DVTM16]. We also were inspired by cylindrical folded origami flashers which expand into a flat circle - examples of which Tom Hull showed in class. Since we need to accommodate for material thickness, we experimented with a flasher, which is Type 2. Through Lincoln Labs, we

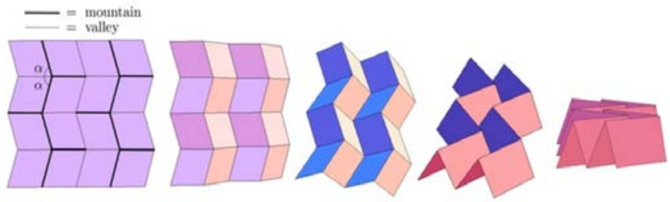

Figure 5: Miura-ori folds. Photo: Tom Hull.

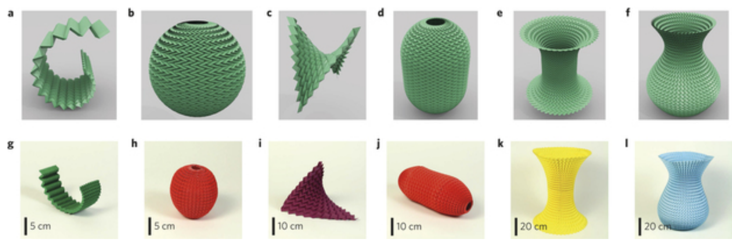

Figure 6: Miura folds on curved surfaces.

have a Mathematica script that generates the crease pattern for flashers of varying numbers of sides and varying material thickness. We were inspired by this method of computationally adapting a crease pattern to the material. We were also inspired by the Hoberman sphere - which has been utilized in Type 2 shelters as in Figure 4 - and compact “auto-open” umbrellas as in Figure 9.

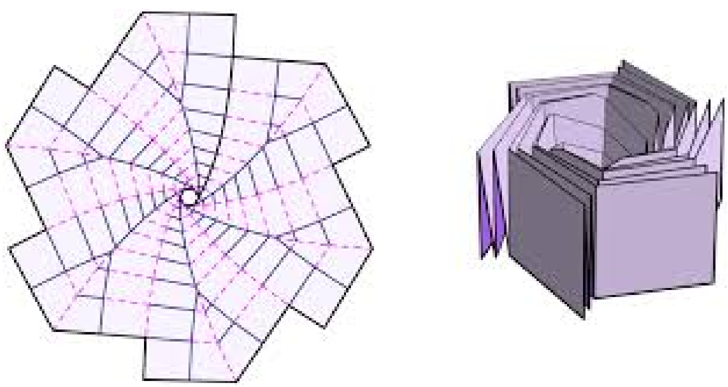

Figure 7: Cylindrical compression flasher.

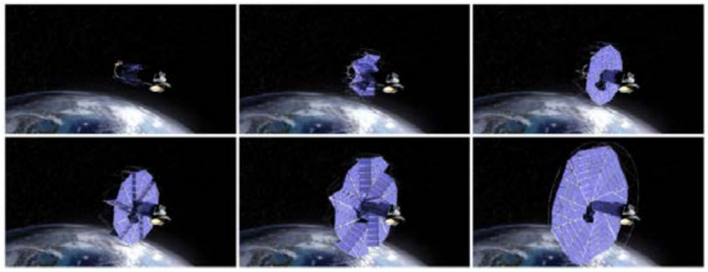

Figure 8: An example of the Miura fold origami flasher utilized for a solar umbrella. [CTS13]

Figure 9: ShedRain umbrella.

3 Approaches

3.1 Hoberman-Inspired Design

Our first approach was to combine a Hoberman half-sphere like in Figure 4 with an origami flasher ground plane, so that the continuous opening motion of the Hoberman would simultaneously deploy the flasher. We protoyped this by tying the flasher at the corners to the Hoberman sphere and pulled it open, as seen in Figure 10. As the Hoberman sphere expanded, it also unfurled the flasher.

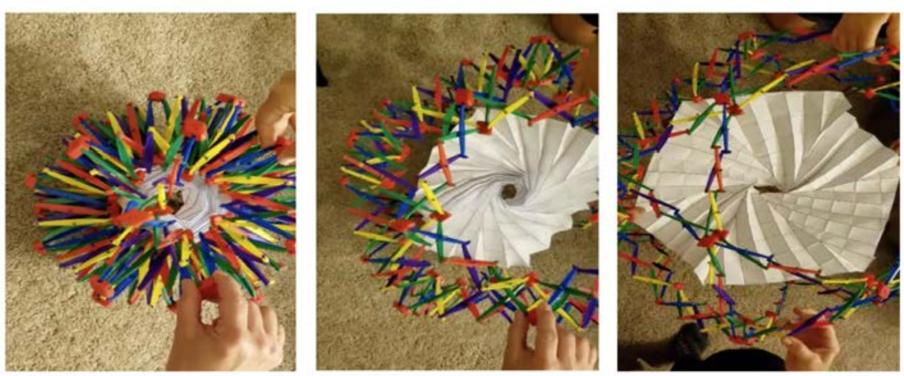

Figure 10: Initial prototype of Hoberman sphere-Flasher hybrid system.

3.2 Umbrella-Inspired Design

We had been interested in auto-open umbrellas since the beginning of the project. One of our initial project ideas had been to make an umbrella that could fold into a very small package. We also became interested in the folding qualities of the umbrella and the connections between the umbrella and the flasher.

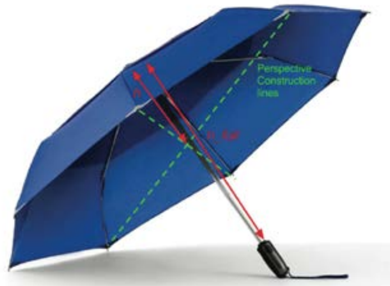

Figure 11

4 Volume Compression Analysis: Hoberman vs Umbrella

Since we had two design routes to choose from, we performed a volume-compression analysis to decide which would yield the greatest volume-compression result. To calculate the volume of the umbrella we will approximate it as a spherical cap of height h and "radius" a (not a true radius of the underlying sphere). Tabulated below are the results of measurements we performed on various commercial Hoberman spheres, a flasher and an umbrella. The purpose of this was to examine what type of volume compression we obtained along with which dimensions (and by how much) were changed in going from a undeployed state to an deployed state..

	Linear Dimensions Undeployed [cm]	Linear Dimensions Deployed [cm]	Linear Ratio	Volume Undeployed [cm^3]	Volume Deployed [cm^3]	Volumetric Ratio
Hoberman Mini	12.7	30.48	42%	1072.53	14,826.67	7.2%
Hoberman Original	22.86	76.20	30%	6,255	2.32×10^5	2.7%
Hoberman Mega	43.18 - 48.26	137.16	31.5% - 35%	42096.2 − 58851.91	1.35×10^6	3.1% - 4.4%
Hoberman Ratio Average			35.1			4.6
Flasher [Cylinder to Flat 2D]	$R \times H = 6x4.5$	$R \times H = 36 \times$ flat 2D	$R \times H = 17\% \times$ N/A	509	Flat 2D	N/A
Umbrella [Cylinder to Spherical Cap]	$R \times H = 5 \times 26$	$a \times h = 61 \times 25$, $h_f = 61$	$a/R = 12.2$, $h/H = 0.96$, $h_{full}/H = 2.35$	2040	$a, h = 154000$, $a, h_f = 480000$	$a, h = 1.3\%$, $a, h_f = 0.4\%$

Looking at the values above, we observe that the volume compression ratio offered by an umbrella design far exceeds that of the Hoberman Spheres. This fact makes such a design approach very appealing for our back-pack sized dome since it would be more portable and less cumbersome to use. Moreover, an umbrella folds into a shape that is amenable to fitting into a back-pack, compared to a Hoberman hemisphere. We therefore decided to take this approach towards designing our shelter.

5 Early Experimentation on Umbrella Design

Since the umbrella had a better volume compression ratio, we first studied the crease pattern of the umbrella. We overlaid plastic on the umbrella and traced where it seemed to fold (as seen in Figure 12. We found that umbrellas fold up in a pattern quite similar to Miura folds. Specifically two different umbrellas we tested exhibited a radially alternating mountain-valley pattern and at different radii, concentric mountain or valley creases. This pattern is shown in Figure 15.

Figure 12: Left: Overlaying the umbrella with plastic to study the crease pattern. Right: First attempt to create an umbrella crease pattern section.

After deducing the crease pattern of one "leaf" of the umbrella, we joined multiple leaves at the edges to create a circle. We did this experimentation with paper and tape.

When we tried to fold it up, not all the folds would not fold because we did not yet account for the thickness of the material. There were vertices where the paper would self-intersect if it were folded. Thus, we cut away the self-intersecting parts of the polygons and filled in the gap with with tape to simulate hinges. As seen in Figure 13, this design folded and unfolded well.

Figure 13: Early prototype of a coned structure made by trimming away excess paper where the faces self-intersected.

6 Designing an exact flat crease pattern

After showing our crease pattern worked, we created a vectorized crease pattern with exact angles. This crease pattern, shown in Figure 15, is for a flat disk. We designed this crease pattern by doing some calculations, which are discussed next.

6.1 Mathematics for the flat crease pattern

We begin by parameterizing the lengths and angles of the crease pattern. Consider a single triangular leaf of the crease pattern, shown in Figure 14. Let the triangle of total height h, be divided into n sections of equal height, $l = \frac{h}{n}$. Moreover, let there be m triangles total that we will align edge to edge to form a flat m-gon. By design then, the angles of the triangle will be

$$\alpha = \frac{360^\circ}{m}$$

$$\beta = \frac{180° - \alpha}{2}$$

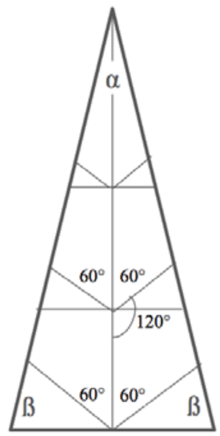

Figure 14: One triangular leaf of the flat crease pattern. We used 60° and 120° angles for our crease patterns for aesthetic reasons, although any angle will still flat-fold.

These equations completely characterize the shape of the triangle that forms one facet of the m-gon but so far we have not added any crease pattern. The crease pattern we reverse-engineered from the umbrella will fold each triangle flat. Additionally when numerous triangles are connected together to form an m-gon we get a "flat" folding that stacks circularly (similar to the aforementioned flashers). This mirrors the behavior of the umbrella as is expected, but this is not restricted to the flexible umbrella material and we can in fact build this using rigid origami (i.e rigid panels and hinges).

Individually looking at each of the vertices where the flat crease pattern (Figure 15) folds, we note that both Kawasaki's and Maekawa's theorems are satisfied simply by the symmetry of the angles in the crease pattern. In fact, for the developable surface, the crease angles could likely be any angle, as long as they satisfy Kawasaki's theorem. To lead credence to this conjecture, we observe visually that this pattern is similar to the popular Miura-fold pattern where one of the dimensions is mapped to a closed loop. Therefore we expect the same range of angles and general limitations to apply in both cases with regards to global flat foldability, although we have not confirmed this result. In fact we postulate the existence of certain types of transformations that maintain global flat foldability although which type has not been explored and is left as a potential future open problem (conformal transformations might be a good candidate due to the fact that maintain local angles).

Both umbrellas tested had the same $60° - 120° - 120° - 60°$ angle distribution at each vertex. We therefore decided to use the same in our crease pattern. All subsequent results rely on using this angle distribution at each vertex. We experimented briefly with other angle distributions and also computed which angle distribution would give the optimal compression ratio. Although as we show the optimal distribution is different to the chosen one, we decided to fabricate using the specified distribution for aesthetic design reasons and to pay homage to the umbrella that formed the inspiration for our design.

6.2 Flat crease pattern prototypes with a rigid material

After getting a precise crease pattern, we then prototyped with a rigid material. We laser cut 1/16" acrylic and fastened it to adhesive vinyl. See Figure 16. Our model expanded and contracted easily. We also noted that we would need to incorporate vertical creases to allow the rigid material to wrap around, like the umbrella.

We also noted that our crease pattern unfolded into a flat disk, while what we wanted was for it to unfold into a dome.

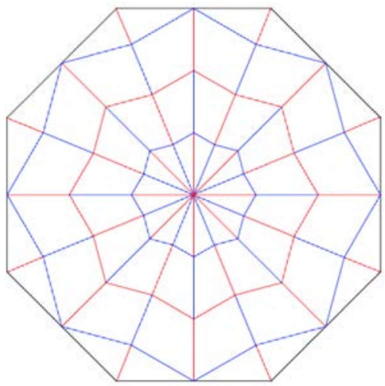

(a) n = 3, m = 8

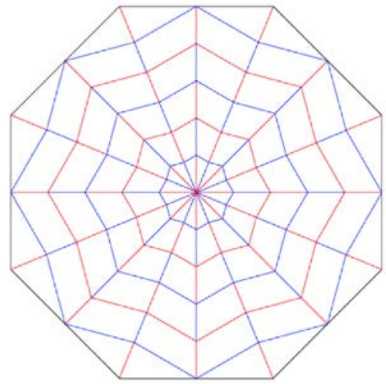

(b) n = 5, m = 8

Figure 15: Crease patterns that deploy into a flat disk.

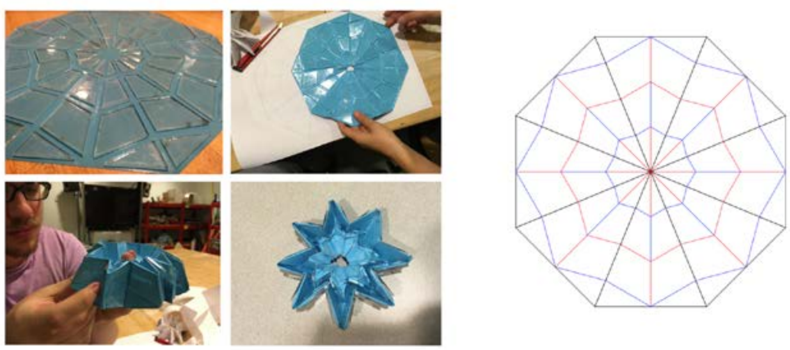

Figure 16: Left: Prototype of rigid structure unfolding flat. Made with acrylic and adhesive vinyl. Right: n = 3, m = 8. Crease pattern referenced to create the prototype.

7 Approximating a hemisphere with rigid material

We wanted to make sure that our design was able to create an inhabitable, 3-dimensional structure. To do this, we were inspired by spherical globe projection which unfolds a curved surface so that it can form a 3-dimensional shape from a flat sheet. See Figure 17.

Having studied the crease pattern of the umbrella we obtained a crease pattern that starts with a flat sheet. This crease pattern has a number of design parameters we adjusted to obtain a crease pattern that fits the surface of a hemisphere. See Figure 15 for the flat crease pattern, and Figure 19 for the hemisphere crease pattern. This type of crease pattern can be modified either deploy flat (developable surface) or be conformed to an arbitrary convex surface - namely the surface of a sphere in our case.

7.1 Mathematics for the hemispherical crease pattern

In our work we focused only on developing rigid origami to approximate a spherical surface, although the underlying mathematics and approach extend to other surfaces as well. In fact the mathematics presented here are inspired by the mathematics of interrupted projection used to print planar maps that are folded into globes or to print designs on curved surfaces.

To begin, refer to Figure 18. Consider a hemisphere of radius r that we wish to approximate using a polyhedron. Let the polyhedron be composed of m leaves or panels that evenly divide the 360° of azimuth each of which is composed of n sections that evenly divide the 90° of inclination angle. The values of n, m, and r will be the parametrization of our dome.

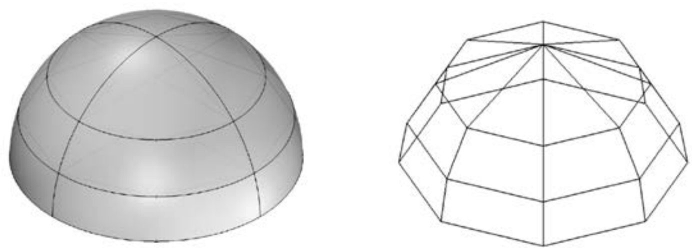

Figure 17: Process of the creation of the final crease patterns. A half dome is partitioned into sections by horizontal planes and then the vertices of the concentric polygons - lying on the surface of the sphere - are connected.

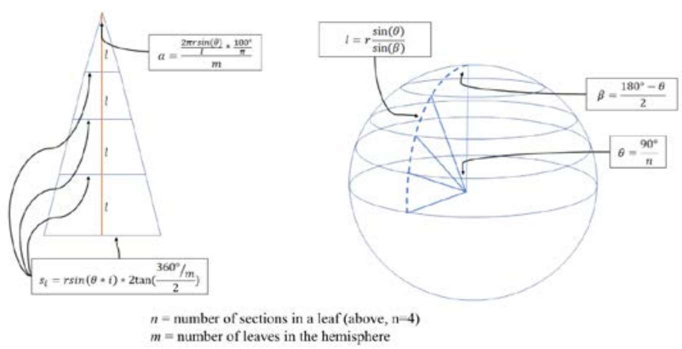

Figure 18
Left: One leaf of the hemisphere; Right: How one leaf lays across the surface of the hemisphere. The dashed line corresponds to the vertical height of one leaf. The l is the same l as shown in the leaf on the left.

$$r \stackrel{\text{def}}{=} \text{radius of the dome}$$
$$n \stackrel{\text{def}}{=} \text{number of sections in a leaf}$$
$$m \stackrel{\text{def}}{=} \text{number of leaves to divide dome into}$$

Suppose we want to place the vertices of our fold pattern for a single leaf, evenly in inclination for a fixed azimuth angle (since this is a single leaf). Each point should then be placed at an angle θ from the previous one, with the first being at an inclination θ and the last at an inclination of $\theta = 90°$, that is the ground. We thus define

$$\theta \stackrel{\text{def}}{=} \frac{90°}{n} \tag{1}$$

The line connecting two vertices (or the first vertex and the top of the dome) together with the two radii extending from the center of the hemisphere to each vertex, form a triangle with θ being one of the angles. Since this triangle is isosceles, the other two angles, ϕ can then simply be defined as

$$\phi \stackrel{\text{def}}{=} \frac{180° - \theta}{2} \tag{2}$$

By using the law of sines we can then compute the height, l of each of the n sections

$$l = r \cdot \frac{\sin\theta}{\sin\phi} \tag{3}$$

While we have chosen the number of leaves and sections in each leaf, we have not discussed the shape of each of the leaves. Since each leaf is part of a polyhedron approximation to a sphere we will approximate each section of the sphere as a trapezoid. The trapezoid at the base of the leaf will be widest and at the top the trapezoid will degenerate into a triangle since all the leaves meet at a point at the pole. At the limit where $n \to \inf$ each of the trapezoids will get very short, i.e $l \to 0$ and approach the exact spherical curvature of the dome.

Similarly, since we have m leaves, at each vertex, the underlying dome we are trying to approximate has a azimuth circle that inscribes a regular m-gon. At each vertex height, the side length of the m-gon is therefore the length, s_i of one of the bases of the trapezoid. Using the radius of the inscribed circle at each vertex height, we can compute all the trapezoid lengths,

$$s_i = r\sin(\theta \cdot i) \cdot 2\tan(\frac{\frac{360^\circ}{m}}{2}) i = 0...n \tag{4}$$

Note that when $i = 0, s_i = 0$ which indicates the top of the triangle section at the top of a leaf. Using these values we can completely characterize the shape of each leaf and hence the final dome. Connecting m such leaves edge to edge as in the flat case is not possible since the edges are not aligned unless folded into the final dome shape. Instead we connect them at the pole by lining up the top triangular edges azimuthally for all m leaves. This results in the "interrupted projection" pattern shown in Figure 19. The full dome is achieved by aligning edges for each of the n sections across all leaves.

7.2 Hemispherical Prototypes

We fabricated two prototypes of our final design out of paper using a plotter and heavy weight paper, one with n=3 and one with n=5. See Figure 19. We verified that our crease pattern did indeed approximate a hemisphere very well.

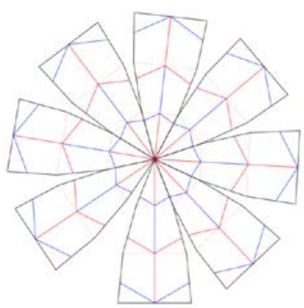

Figure 19: Left: spherical crease pattern; Right: Paper prototype folded from spherical crease pattern, n = 3, m = 8.

8 Flat-folding the hemisphere

At this point, we decided we leave one leaf unconnected to the other, so that the dome would have a cut from the base up to the center. This is where the shelter can open and fold up radially on itself. This would mean we would not need to complicate the crease pattern with additional vertical creases for the rigid material to wrap around. The folded dome now flat-folds into a package, as shown in Figure 20.

8.1 Volume-compression analysis from flat-folded state to deployed hemisphere

We performed some calculations to get the relationship between the dimensions of the folded package and the deployed dome radius. In this configuration, the folded dome can be considered as a stacking of m flat-folded leaves. It therefore suffices to examine the compression of a single leaf.

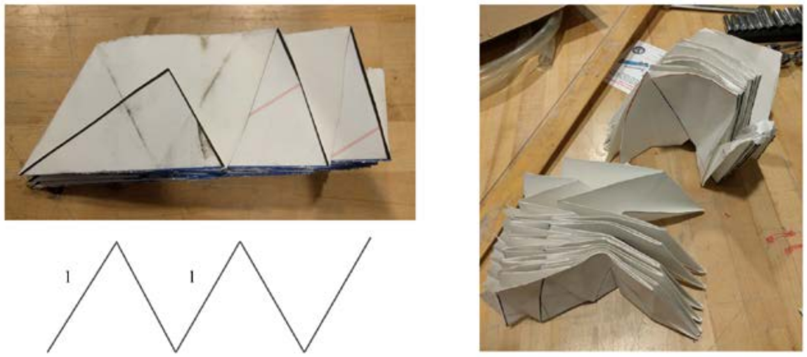

Figure 20

We begin by noting that the concentric creases alternate mountain-valley at each vertex. The effect of this is that if we look at the folded state in "X-ray" view each of the n sections of length l form one side of a triangle. The resulting pattern for $n = 5$ is shown in the bottom left of Figure 20. Reasoning about the same concentric creases and how they fold towards the radial creases allows us to map the angle between these to creases, ψ to one of the angles of the folded crease pattern. Using this observation we can compute the compressed height, h_c and compressed length, l_c, for a chosen n and r.

$$h_c(n, r) = l \sin(\psi) = r \cdot \frac{\sin\theta}{\sin\phi} \cdot \sin(\psi) \tag{5}$$

$$l_c(n, r) = n \cdot l \cos(\psi) = n \cdot r \cdot \frac{\sin\theta}{\sin\phi} \cdot \cos(\psi) \tag{6}$$

Note that this result is dependent on all vertices having the same angle distribution around them. This need not be the case and would change the result for h_c and l_c, however We did not explore this case. Regardless though the observation that the each of the n sections would form the side of a triangle with length l would still hold true.

We do not have a general bound on the compressed thickness t_c of the final package. That said, the final result is ultimately dependent on how many layers overlap at the thickest point of the folded state of the leaf (this thickest point will by design be at a vertex). Each of the n sections contributes at most 2 layers on either side of a vertex. These observations can serve as the basis to obtain a more general result for t_c that would depend on ψ.

Assuming the effects on t_c don't vary much with ψ, the optimal value ψ^* that minimizes the compressed volume can be obtained by looking at the product $h_c \cdot t_c$. We therefore get

$$\psi^* = \arg\min_{\psi} |n \cdot l^2 \cos(\psi) \sin(\psi)| = 0°, 90° \tag{7}$$

Note that both 0° and 90° represent a degenerate case. While indeed the package folds flat it can't align properly with adjacent pieces. Therefore we would need a full equation for t_c so as to find psi^*. We will therefore restrict ourselves to looking explicitly at our chosen angle distribution.

For our chosen angle distribution, we have calculated results for the compressed height h'_c, length l'_c and thickness t_c of the package. This causes the triangles that are formed by the sections to be equilateral, yielding the following relations

$$l'_c(n, r) = \frac{nl}{2} = \frac{nr}{2} \frac{sin(\frac{90}{n})}{sin(\frac{180-\theta}{2})} \tag{8}$$

$$h'_c(n, r) = \frac{\sqrt{3}}{2} l = \frac{\sqrt{3}}{2} r \frac{sin(\frac{90}{n})}{sin(\frac{180-\theta}{2})} \tag{9}$$

$$t'_c(n, m, t_{material}) = (2 \left\lceil \frac{n}{2} \right\rceil + 2) \cdot m \cdot t_{material} \tag{10}$$

For $n = 5, m = 8$ we can obtain approximate values for the above.

$$l'_c(n \geq 2, r) \approx \frac{pi}{4} r \approx 0.785r$$
$$h'_c(n = 5, r) \approx 0.271r$$
$$t'_c(n = 5, m = 8, t_{material}) = 64t_{material}$$

Which for our designed dome, with $n = 5, m = 8, r = 0.5m, t_{material} = 0.15875cm$ and an angle distribution at the vertices of $60° - 120° - 120° - 60°$ we obtain compressed dimensions of

$$l'_c = 0.393m$$
$$h'_c = 0.136m$$
$$t'_c = 0.10m$$

Which results in a compressed volume, V_c and volume ratio of

$$V'_c = l'_c h'_c t'_c \approx 0.00543m^3$$
$$V = \frac{2}{3}\pi r^3 \approx 0.262m^3$$

$$\boxed{\frac{V_c}{V} = 2.1\%}$$

Note that since t'_c is independent of the radius and h_c and l_c scale fractionally with radius (i.e linear coefficient of < 1), we in fact expect the compression ratio $\frac{V'_c}{V}$ to decrease with increased radius of the desired dome.

9 Final Design and Fabrication

After many prototypes, we constructed our final product: a model with 1m diameter made of acrylic faces sandwiched between sheets of vinyl. We laser cut our design with 1/16" acrylic, leaving 1/8" gaps to allow the material to fold. We positioned the rigid faces on vinyl using the negative of our design (leftover from laser cutting) to ensure proper spacing, as seen in Figure 21.

Figure 21: Acrylic stencil used to place the laser cut rigid faces on vinyl.

We attached velcro to the cut edge– the edge which allows the dome to flat-fold radially– so that we would be able to close the dome. We found that the final deployed dome can stand on its own without any internal support, which was a pleasant surprise. It supports itself similar to an arch, where each face supports its neighbors. The deployment was harder than expected, due to imperfect construction techniques.

(a) The final structure in its folded form.

(b) The final structure unfolding.

Figure 23: The final construction.

10 Future Work

There are a few directions we could expand on to extend our project:

- Web app to generate crease pattern. Since we have a computational, standardized protocol for the creation of Miura-compression crease patterns from 3D domes, we could potentially create a web app in which a 3D convex surface design could be input to generate a crease pattern for a Miura-compression foldable shelter. The user could specify the number of leaves m, number of sections on each leaf n, desired radius of the dome (or if we allow non-hemisphere shapes, the surface they would like to approximate), material thickness, and the folding angle *psi*. The web app would then live-update with the new crease pattern, a model of the folded package and its dimensions, and the volume compression ratio.
- Adding hinges. In the future, we could also implement the design of hinges to aid the structures in deploying more smoothly. Hinges might help bias folds to mountain or valley, and restrict their range of motion to the crease angle that we want. This would help the shelter deploy and fold more easily. We did buy some spring-loaded hinges, which we could fasten to the creases and could also help with deployment.
- Deployment mechanism. We could design a mechanical way to fold and unfold the structure easily. Potential ideas we had included an umbrella-like mechanism (a central telescoping pole with metal struts), a Hoberman-like expanding hemisphere, or a central telescoping pole with an expanding 2D circle along the base perimeter.

Appendices

A Matlab script to approximate the sphere as a regular polyhedron

```
n=3;
m=8;
r=3;

inclination = 90/n;
face_angle = (180 - inclination)/2; %
face_length = r*(sind(inclination)/sind(face_angle));

h_cone = face_length*cosd(face_angle);
r_cone = face_length*sind(face_angle);
cone_sector_angle = rad2deg(2*pi*r_cone/face_length);
alpha = cone_sector_angle / m;

i=0:n;
si = 2*(r*sind(inclination*i))*tand(180/m);
si_half = si./2;
delta_si_half = diff(si_half);
beta_i = zeros(1,2*n-1);
beta_i(1) = (180-alpha)/2;
beta(3:2:end) = atan2d(face_length,(si_half(3:2:end)-si_half(2:2:end-1)));
beta(2:2:end-1) = 180 - beta(3:2:end);

full_face_angles = beta(1:2:end-2)+beta(2:2:end-1);
```

References

[CTS13] Michael T Contreras, Brian P Trease, and Brent Sherwood. The solar umbrella: A low-cost demonstration of scalable space based solar power. In *Wireless for Space and Extreme Environments (WiSEE), 2013 IEEE International Conference on*, pages 1–6. IEEE, 2013.

[DVTM16] Levi H Dudte, Etienne Vouga, Tomohiro Tachi, and L Mahadevan. Programming curvature using origami tessellations. *Nature materials*, 2016.

[Kim11] Hwang Kim. Urban homeless cocoon, Mar 2011.

[Tac] Tomohiro Tachi. Rigid-foldable origami gallery.